ELSEVIER

Journal of Molecular Structure (Theochem) 545 (2001) 29–47

THEO CHEM

www.elsevier.nl/locate/theochem

An ab initio exploratory study of side chain conformations for selected backbone conformations of *N*-acetyl-L-glutamine-*N*-methylamide

A.M. Tarditi[a], M.W. Klipfel[a], A.M. Rodriguez[a,*], F.D. Suvire[a], G.A. Chasse[a,b], O. Farkas[c], A. Perczel[c], R.D. Enriz[a]

[a]*Department of Chemistry, National University of San Luis, Chacabuco 915, 5700 San Luis, Argentina*
[b]*Department of Chemistry, University of Toronto, Toronto, Ontario, Canada M5S 3H6*
[c]*Institute of Organic Chemistry, Eotvos University, P.O. Box 32, H-1117 112 Budapest, Hungary*

Received 24 November 2000; accepted 27 November 2000

Abstract

The backbone potential energy surface (PES) (Ramachandran map) of *N*-acetyl-L-glutamine-*N*-methylamide has been studied at a,a side-chain orientation. Side-chain PESs at selected backbone conformations (γ_L and β_L) were also studied. Side-chain–backbone interactions were analyzed in terms of energy and geometry.

Keywords: Side-chain orientation in glutamine; Side-chain–backbone interactions; Ab initio MO study; Peptide conformations; Ramachandran map of glutamine residue

1. Introduction

Glutamine is found in the human body in greater abundance than any other free amino acid. It is crucial for many aspects of healthy body function. It is necessary for the maintenance of optimal antioxidant status since it is part of gluthathion, which is one of the body's most important antioxidants against oxidative stress. It has a crucial role to play in the maintenance of optimal immune function since glutamine is a nutrient for secretory immunoglobulin A (sIgA) producing cells. It is also important for the building and maintenance of muscle and intestinal tissues.

Glutamine is a higher homolog of asparagine since glutamine has two CH_2 groups in its side-chain while asparagine has only one. This also implies that the glutamine side-chain can reach further out than that of asparagine. For this reason, glutamine in a protein has not only structural but a functional role to play as well.

In this respect, it is important to mention that the glutamine residue, as part of a certain protein has an important role to play in blood-clotting. Laki and Lorand, discovered [1] "*blood coagulation factor XIII*" in 1948. It has been shown [2–6] later that Factor XIII is a proenzyme (pro-transglutaminase) from which transglutaminase is produced. Transglutaminase, which is involved in blood-clotting,

* Corresponding author.
E-mail addresses: atarditti@unsl.edu.ar (A.M. Tarditi), mklipfel@unsl.edu.ar (M.W. Klipfel), amrodri@unsl.edu.ar (A.M. Rodriguez), gchasse@fixy.org (G.A. Chasse), farkas@para.chem.elte.hu (O. Farkas), perczel@para.chem.elte.hu (A. Perczel), denriz@unsl.edu.ar (R.D. Enriz).

0166-1280/01/$ - see front matter
PII: S0166-1280(01)00352-9

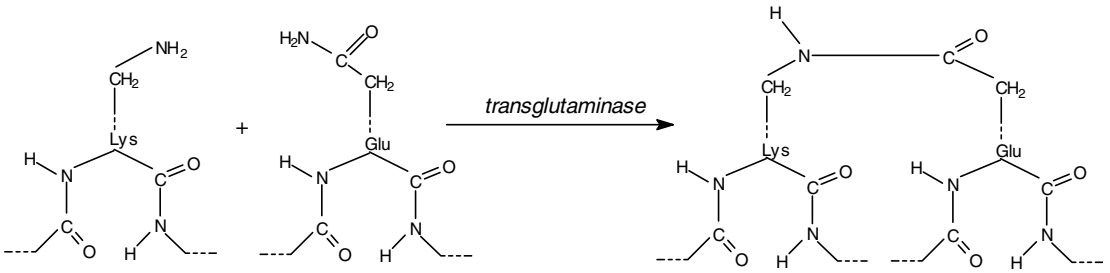

Scheme 1.

analogous to cysteine proteases, after the activation of the proenzyme, joins the side-chains of Lys and Glu forming cross-linkages between protein molecules such as fibrin and antiplasmin [7] (cf. Scheme 1 (a schematic illustration of the reaction catalyzed by transglutaminase, which plays a pivotal in blood clotting)). Factor XIII also occurs in human monocytes [8], not only in blood plasma. The 3D X-ray structure of the proenzyme became known [9] since 1994. This field has been reviewed extensively [10]. Glutamine is also used in the food industry as a browning inhibitor for the "black spot" phenomenon produced by *Carnimonas nigrificans* [11].

In the case of glutamine, the side chain may be mimicked by butanamide (**I**). The terminal CH_3 group in **I** corresponds to the α-carbon of *N*-acetyl-L-glutamine-*N*-methylamide (**II**):

Table 1
Definition of key-torsional angles for butanamide (**I**) and *N*-acetyl-L-glutamine-*N*-methylamide (**II**)

Dihedral angle	Molecule	
	Butanamide (*I*)	*N*-acetyl-L-glutamine-*N*-methylamide (**II**)
χ_1	$H^7–C^1–C^2–C^3$	$N^1–C^2–C^7–C^8$
χ_2	$C^1–C^2–C^3–C^4$	$C^2–C^7–C^8–C^9$
χ_3	$C^2–C^3–C^4–O^5$	$C^7–C^8–C^9–N^{11}$
χ_4	$C^3–C^4–N^5–H^{14}$	$C^8–C^9–N^{11}–H^{16}$
ω_0	–	$C^{19}–C^{18}–N^1–C^2$
ω_1	–	$C^2–C^3–N^{24}–C^{25}$
ϕ	–	$C^{18}–N^1–C^2–C^3$
ψ	–	$N^1–C^2–C^3–N^{24}$

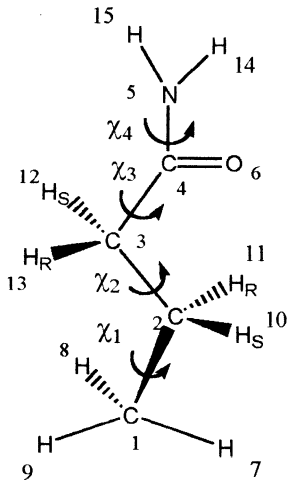

I

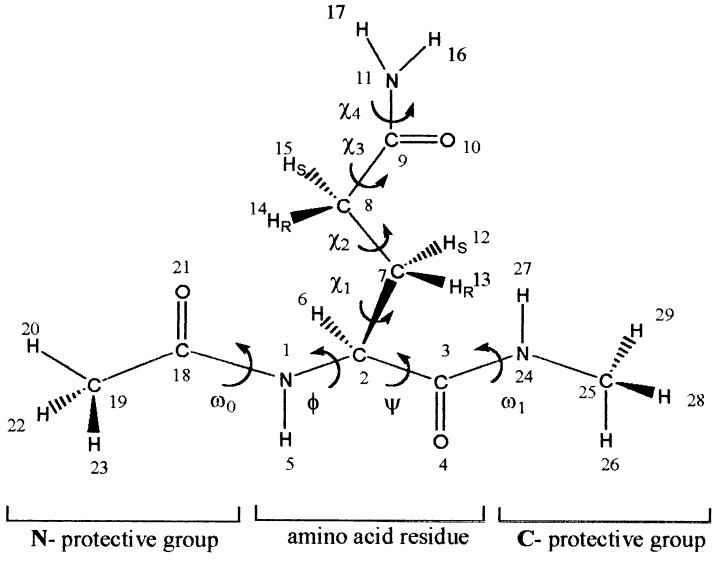

II

Clearly, such comparison is similar to that of the previous study [12] where propanamide (**III**) is used to model the side chain of N- and C-protected asparagine (**IV**):

Consequently, the extra CH_2 group increases the number of torsional angles from two to three. This implies that for **I** and **II** we have a PEHS (Eq. (1)) in terms of χ_1, χ_2 and χ_3 while for **III** and **IV**, the

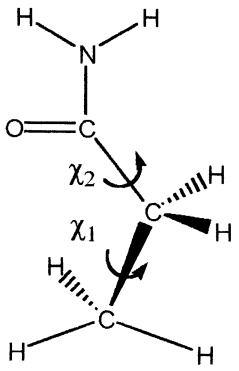

III

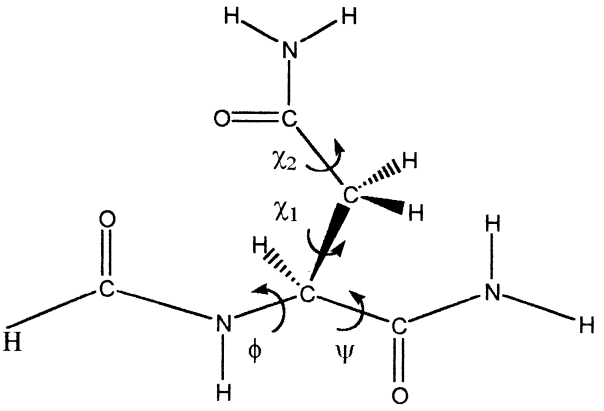

IV

Table 2
Total energy values of the component molecules for isodesmic reaction computed at the level of theory RHF/3-21G

	Molecular system	Energy (hartree)
Me–CONH–CH_2–CONH–Me	γ_L	−451.2942433
	β_L	−451.2931883
CH_3–R	R = H	−39.976877
	R = –CH_2–CH_2–$CONH_2$	−284.4581386

Table 3
Optimized torsional angles, total energy values and relative energies for the conformational minima of butanamide computed of the RHF/3-21G level of theory

Initial conformations		Optimized parameters			
χ_2	χ_3	χ_2	χ_3	Total energy (hartree)	ΔE (kcal/mol)
g^+	g^+	68.78	86.3	−284.4554062	1.71
g^+	a	70.05	187.23	−284.4581386	0.00
g^+	g^-	Not found			
a	g^+	167.66	73.21	−284.4547564	2.12
a	a	180.00	180.00	−284.4572082	0.58
a	g^-	−177.66	−73.20	−284.4547565	2.12
g^-	g^+	Not found			
g^-	a	−70.05	172.76	−284.4581386	0.00
g^-	g^-	−68.72	−86.12	−284.4554061	1.71

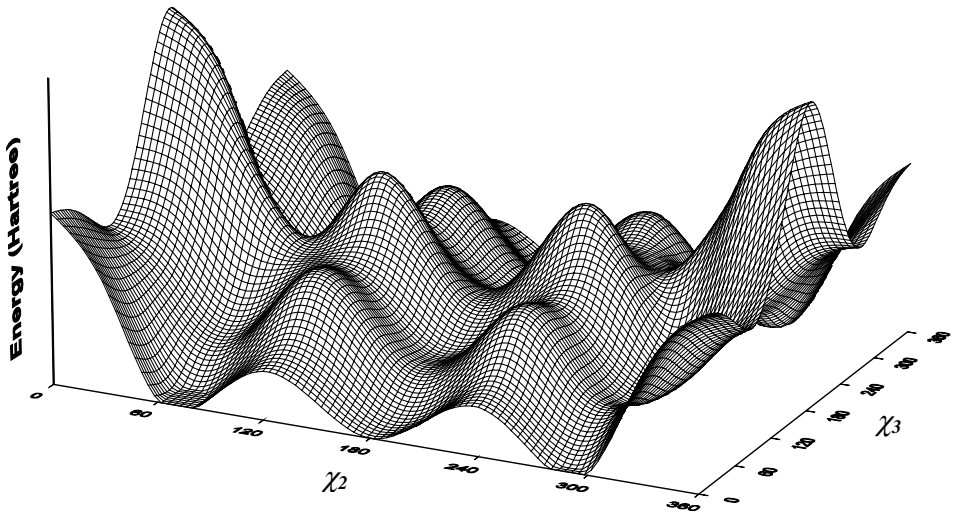

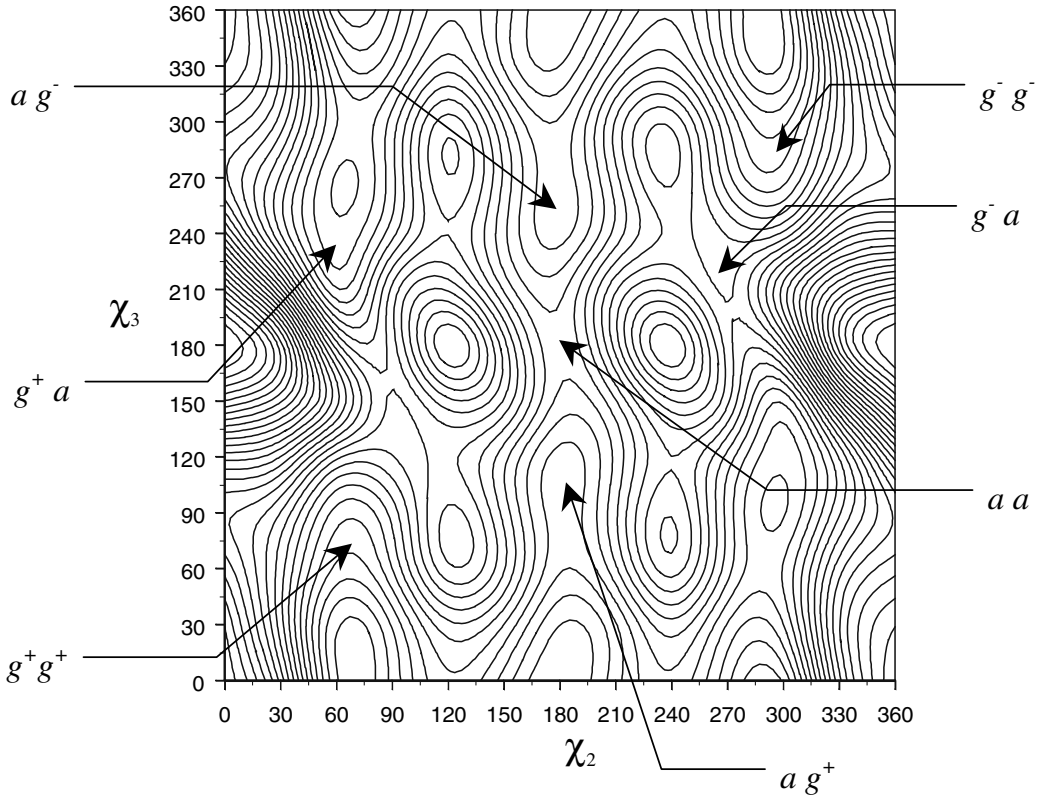

Fig. 1. Conformational PES, $E = E(\chi_2;\chi_3)$, for butanamide CH_3–(χ_1)–CH_2–(χ_2)–CH_2–(χ_3)–$CONH_2$.

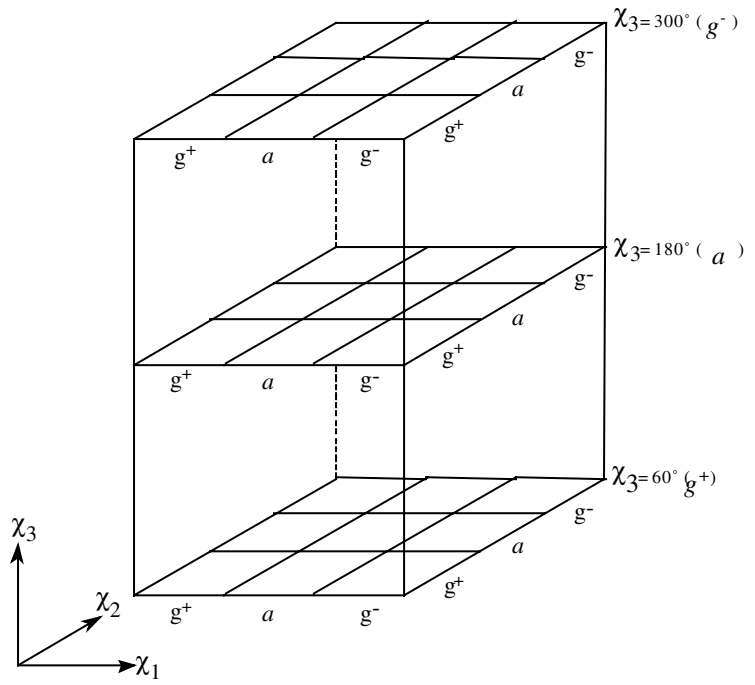

Fig. 2. Three potential energy surface (PES) cross-sections, $E(\chi_1,\chi_2)$, of a potential energy hypersurface (PEHS): $E(\chi_1,\chi_2,\chi_3)$. The levels correspond to $\chi_3 = g^+$, $\chi_3 = a$, and $\chi_3 = g^-$ on going from bottom to top.

energy is a function (Eq. (2)) of only two independent variables χ_1 and χ_2:

$$E = E(\chi_1, \chi_2, \chi_3) \qquad \text{PEHS for } \mathbf{I} \text{ and } \mathbf{II} \tag{1}$$

$$E = E(\chi_1, \chi_2) \qquad \text{PES for } \mathbf{III} \text{ and } \mathbf{IV} \tag{2}$$

Previous study [12] indicated that the amide rotation (χ_2 in **III**) has three minima (g + , a, g −) with the *anti* orientation being the most stable. In view of this

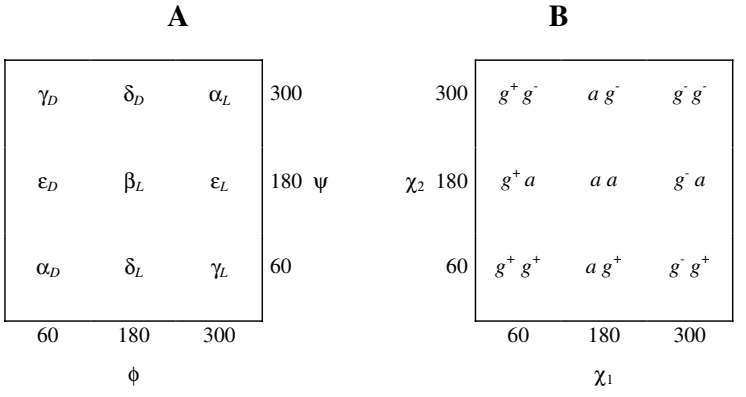

Fig. 3. Topology of the backbone or Ramachandran (A) and a double rotor side-chain (B) potential energy surfaces (PES) as cross-sections of a potential energy hypersurfaces (PEHS) of four independent variables: $E_{\chi 3=syn} = E(\phi, \psi, \chi_1, \chi_2)$. Such a PEHS is applicable for all *trans*-peptide bond ($\omega_0 = \omega_1 = 180°$) containing glutamine residue in a peptide chain with a *syn* orientation of the amide moiety.

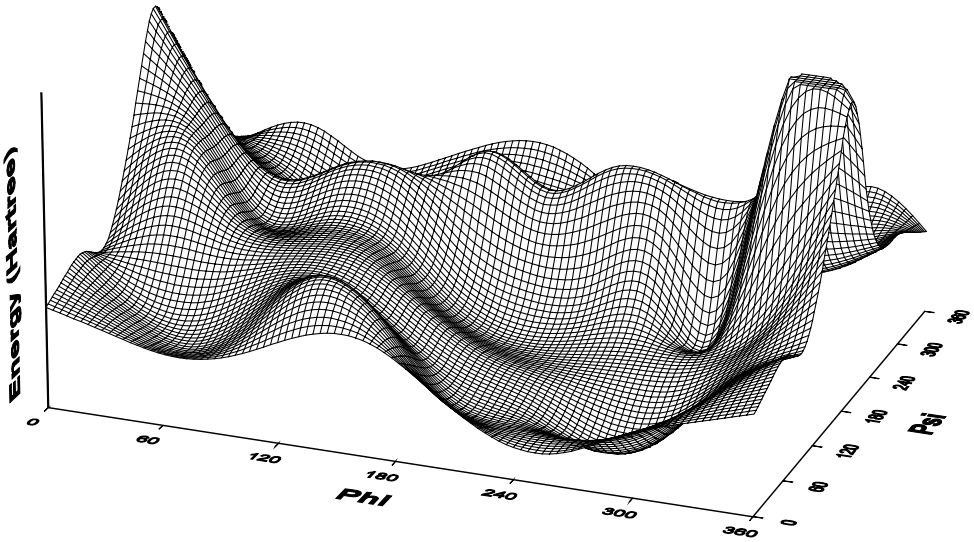

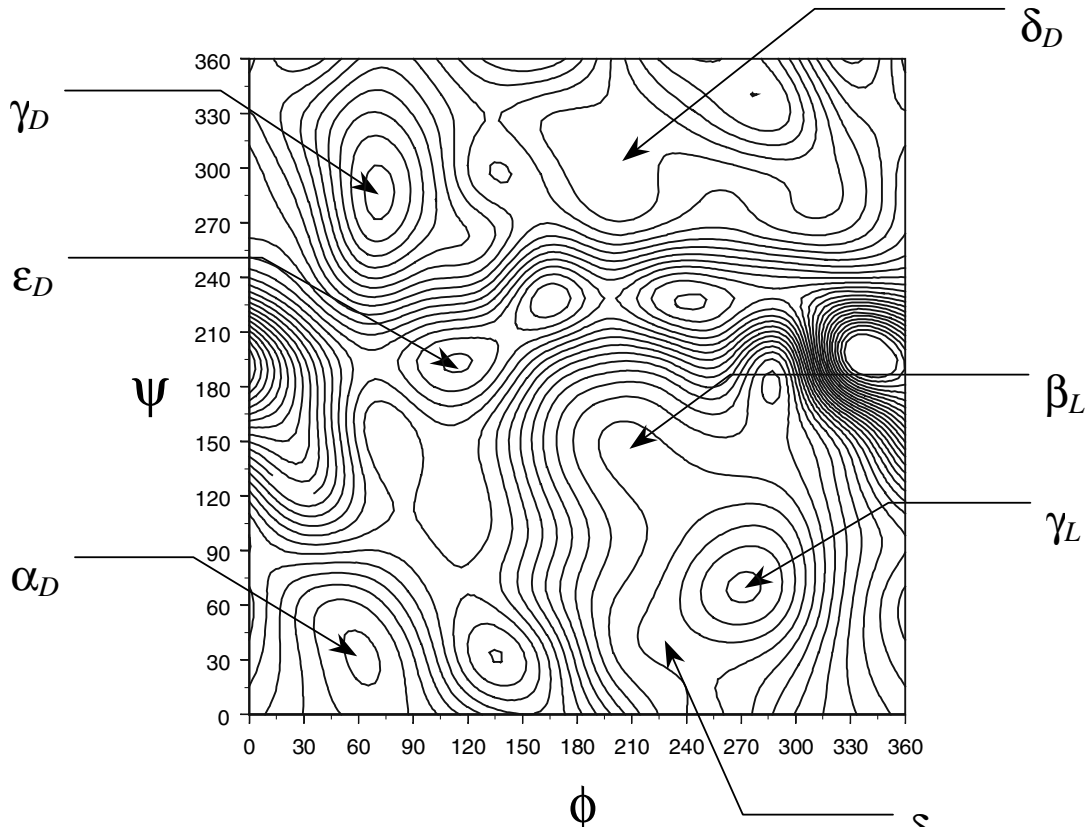

Fig. 4. Ramachandran PES for *N*-acetyl-L-glutamine-*N*-methylamide.

Table 4
All backbone (BB) conformations of *N*-acetyl-L-glutamine-*N*-methyl amide for the fully *anti* side chain (SC) orientation optimized at RHF/3-21G level of theory

	ϕ	ψ	ω_0	ω_1	χ_1	χ_2	χ_3	Total energy (hartree)	ΔE[a] (kcal mol^{-1})	$\Delta E_{\text{stabil.}}$ (γ_L) (kcal mol^{-1})	ΔE_{stabil}·(β_L) (kcal mol^{-1})
α_D	60.50	38.18	−165.64	−179.91	−167.13	−164.05	157.69	−695.776020	14.32	−0.32	−0.34
ε_D	70.50	163.34	−170.87	176.48	−164.37	−161.57	152.18	−695.764213	21.73	7.09	7.75
γ_D	73.03	−53.90	174.71	−175.51	−178.60	161.58	168.24	−695.779799	11.94	−2.68	−2.02
δ_L	−127.22	28.83	−170.89	176.55	−164.37	174.43	173.89	−695.776935	13.74	−0.90	1.55
β_L	−160.26	152.40	−179.01	−178.46	−173.68	179.86	−174.68	−695.778231	12.93	−1.71	−1.05
δ_D	−173.60	−42.35	173.17	−178.09	−171.98	159.43	−166.05	−695.773910	15.64	1.00	1.66
α_L				Not found (goes to δ_L)							
ε_L				Not found (goes to γ_L)							
α_L	−85.75	68.06	−179.03	178.78	−173.59	179.82	−174.70	−695.786269	7.88	−6.75	−7.41

[a] The global minimum corresponds to β_L (g^-, g^-) conformation having −695.7988342 hartree total energy. These values is taken a reference value, corresponding to relative energy 0.00 kcal mol^{-1}.

Table 5
Optimized torsional angles, total energy values, relative energies and stabilizations energies, for the conformational minima of *N*-acetyl-L-glutamine-*N*-methylamide in its (γ_L) backbone conformation, computed at the RHF/3-21G level of theory

Initial conformations			Optimized parameters										
χ_1	χ_2	χ_3	χ_1	χ_2	χ_3	ϕ	ψ	ω_0	ω_1	Total energy (hartree)	ΔE^a (kcal mol^{-1})	ΔE_{stabil} (γ_L) (kcal mol^{-1})	ΔE_{stabil} (β_L) (kcal mol^{-1})
g^+	g^+	*a*	69.63	105.84	−152.59	−85.16	72.13	−174.35	−178.75	−695.7803174	11.63	−3.02	−3.68
g^+	a	a	64.10	−169.14	−160.94	−85.13	64.58	−172.76	−179.59	−695.7836468	9.53	−5.11	−5.77
g^+	g^-	a	69.13	−81.63	−160.37	−82.72	62.42	−171.97	−179.53	−695.7973782	0.91	−13.73	−14.39
a	g^+	a	−175.86	66.29	169.63	−86.06	68.40	−173.03	−178.67	−695.7878075	6.88	−7.72	−8.38
a	a	a	−174.66	171.45	169.63	−85.86	68.05	−174.21	−178.46	−695.7862686	7.89	−6.75	−7.41
a	g^-	a	175.02	−109.96	151.97	−85.84	63.75	−174.44	−178.89	−695.7809096	11.25	−3.39	−4.05
g^-	g^+	a	−58.91	89.99	161.25	−85.53	65.36	−174.91	−178.86	−695.7939801	3.05	−11.59	−12.25
g^-	a	a	−68.88	161.66	156.76	−86.16	66.99	−177.13	−178.83	−695.7822974	10.38	−4.26	−4.92
g^-	g^-	a	−63.88	−69.73	−178.22	−86.48	70.35	−177.90	−178.92	−695.7846939	8.00	−5.77	−6.43

[a] The global minimum corresponds to β_L (g^-, g^-) conformation having −695.7988342 hartree total energy. These values is taken a reference value, corresponding to relative energy 0.00 kcal mol^{-1}.

Table 6
Optimized torsional angles, total energy values, relative energies and stabilizations energies, for the conformational minima of *N*-acetyl-L-glutamine-*N*-methylamide in its (β_L) backbone conformation, computed at the RHF/3-21G level of theory

Initial conformations			Optimized parameters										
χ_1	χ_2	χ_3	χ_1	χ_2	χ_3	ϕ	ψ	ω_0	ω_1	Total energy (hartree)	ΔE (kcal mol^{-1})	ΔE_{stabil} (γ_L) (kcal mol^{-1})	ΔE_{stabil} (β_L) (kcal mol^{-1})
g^+	g^+	*a*	60.15	86.76	190.83	−167.05	157.74	182.39	167.69	−695.7860592	8.02	−6.62	−7.28
g^+	a	a	53.64	158.49	164.33	−166.55	165.02	−182.09	176.17	−695.7834871	9.63	−5.01	−5.67
g^+	g^-	a	64.54	−62.9	114.14	−169.68	154.97	−168.03	176.35	−695.7869796	7.44	−7.20	−7.86
a	g^+	a	−178.37	54.66	94.42	−166.46	160.03	177.73	−179.72	−695.7940775	2.98	−11.65	−12.31
a	a	a	−173.68	179.86	−174.68	−160.27	152.42	−179.01	178.77	−695.7782313	12.93	−1.71	−2.37
a	g^-	a	−174.89	−84.64	163.99	−160.26	152.40	−179.90	172.85	−695.7777517	13.22	−1.41	−2.07
g^-	g^+	a	−69.37	86.48	−175.5	−159.37	162.64	−172.4	177.21	−695.7835429	9.59	−5.04	−5.70
g^-	a	a	−59.37	−155.97	−169.69	−145.93	168.27	−172.67	177.11	−695.7829040	9.99	−4.64	−5.30
g^-	g^-	a	−101.82	−69.91	−177.93	−164.41	171.69	175.51	179.86	−695.7988342	0.00	−14.64	−16.30

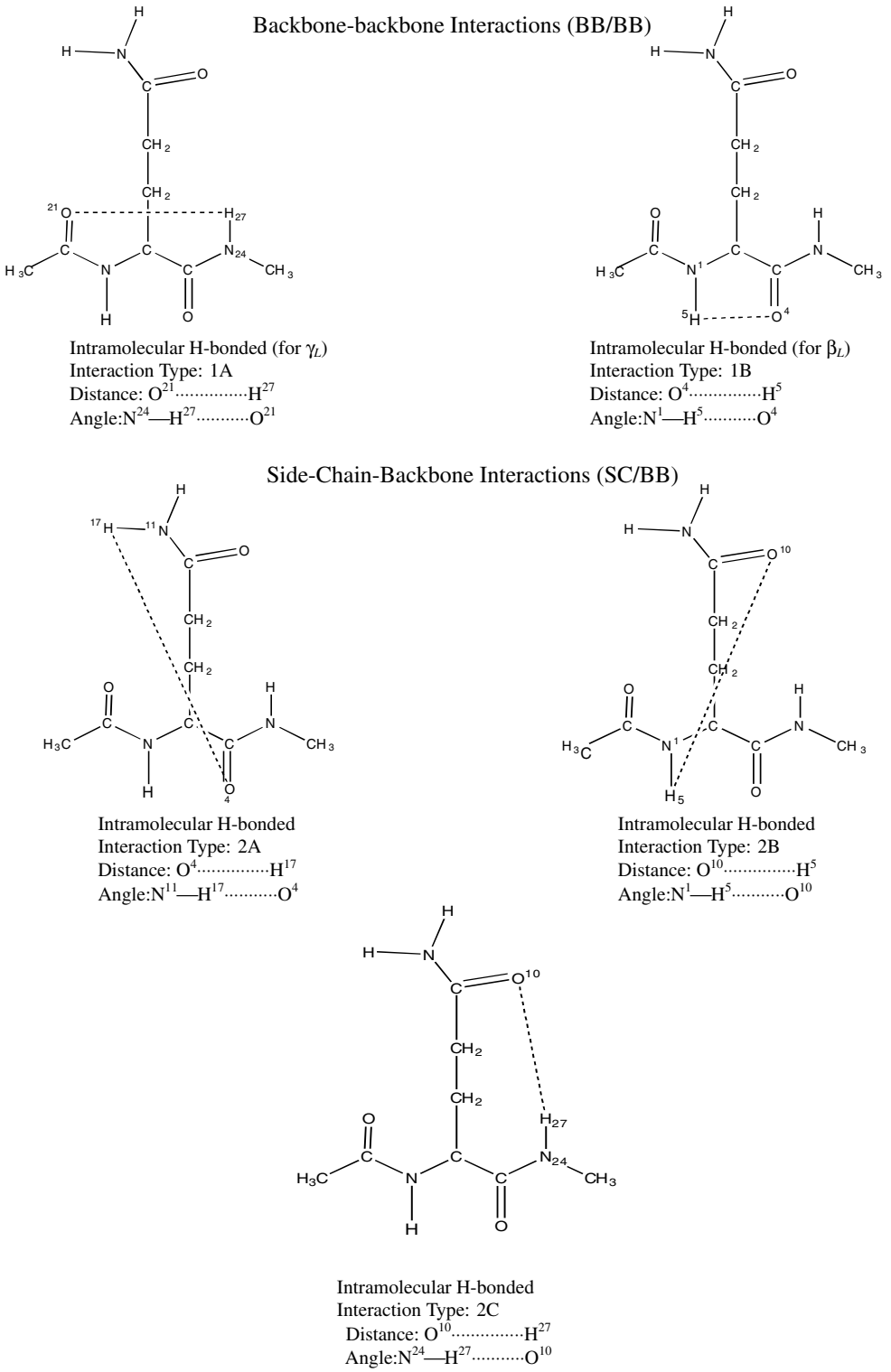

Fig. 5. Classification of various types of BB/BB and SC/BB interaction.

Table 7
Summary of intramolecular interactions in *N*-acetyl-L-glutamine-*N*-methylamide

Conformations	Energy (hartree)	$\Delta E_{rel.}$ (kcal mol^{-1})	Interaction type		Distance (Å)	Angle (°)
			BB/BB	SC/BB		
α_D (a, a)	−695.7760201	14.32	–	–	–	–
ε_D (a, a)	−695.7642131	21.73	–	–	–	–
γ_D (a, a)	−695.7797999	11.94	1A	–	1.88	149.90
δ_L (a, a)	−695.7769355	13.74	–	–	–	–
δ_D (a, a)	−695.7739096	12.93	–	–	–	–
β_L (g^+, g–)	−695.7860592	8.02	1B	–	2.12	108.36
β_L (g^+, a)	−695.7834871	9.63	1B	–	2.13	108.26
β_L (g^+, g^-)	−695.7869796	7.44	1B	–	2.28	104.18
			–	2A	2.22	133.00
β_L (a, g^+)	−695.7940775	2.98	1B	–	2.10	109.32
			–	2C	1.91	158.41
β_L (a, a)	−695.7782313	12.93	1B	–	2.18	106.26
β_D (a, g^-)	−695.7777517	13.22	1B	–	2.17	106.67
β_D (g^-, g^+)	−695.7835429	9.59	1B	–	2.19	104.99
β_D (g^-, a)	−695.7829040	9.99	1B	–	2.14	107.32
β_D (g^-, g^-)	**−695.7988342**	**0.00**	1B	–	1.94	110.54
			–	2C	1.94	159.43
γ_L (g^+, g^+)	−695.7803174	11.62				
γ_L (g^+, a)	−695.7836468	9.53	1A	–	1.97	146.28
γ_D (g^+, g^-)	−695.7973782	0.91	1A	–	1.90	148.67
			–	2B	1.77	158.37
γ_L (a, g^+)	−695.7878075	6.88	1A	–	1.99	146.34
γ_L (a, a)	−695.7862686	7.89	1A	–	2.00	144.56
γ_L (a, g^-)	−695.7809096	11.25	1A	–	1.99	146.34
γ_L (g^-, g +)	−695.7939801	3.05	1A	–	1.95	146.55
			–	2B	1.87	147.14
γ_L (g^-, a)	−695.7822974	10.38	1A	–	2.04	144.05
γ_L (g^-, g^-)	−695.7846939	8.00	1A	–	2.08	141.57

we may partition Eq. (1) into three potential energy surfaces (PESs) of two independent variables:

$$E_{\chi_{3=g+}} = E(\chi_1, \chi_2) \quad \text{for PEHS for } \mathbf{I} \text{ and } \mathbf{II}\ (\chi_3 = g^+) \tag{3a}$$

$$E_{\chi_{3=a}} = E(\chi_1, \chi_2) \quad \text{for PEHS for } \mathbf{I} \text{ and } \mathbf{II}\ (\chi_3 = a) \tag{3b}$$

$$E_{\chi_{3=g-}} = E(\chi_1, \chi_2) \quad \text{for PEHS for } \mathbf{I} \text{ and } \mathbf{II}\ (\chi_3 = g^-) \tag{3c}$$

However, due to the fact the *anti* orientation is the most stable, we will limit our consideration to Eq. (3b) only.

2. Method

2.1. Conformational analysis

In the modular approach, the numbering of the atoms of each amino acid residues are done together and the N- as well as the C-protective groups are also done separately. This method may lend itself to easy extension to oligopeptides so that each amino acid residue in the oligopeptide could easily be compared to the amino acid residue in the diamide. The numbering system is shown in **II**. The definitions at key torsional angles associated with peptide folding, are summarized in Table 1.

In accordance with the IUPAC-IUB [13] recommendation dihedral or torsional angles were specified (Eq. (4)) within −180 and 180° for both backbone

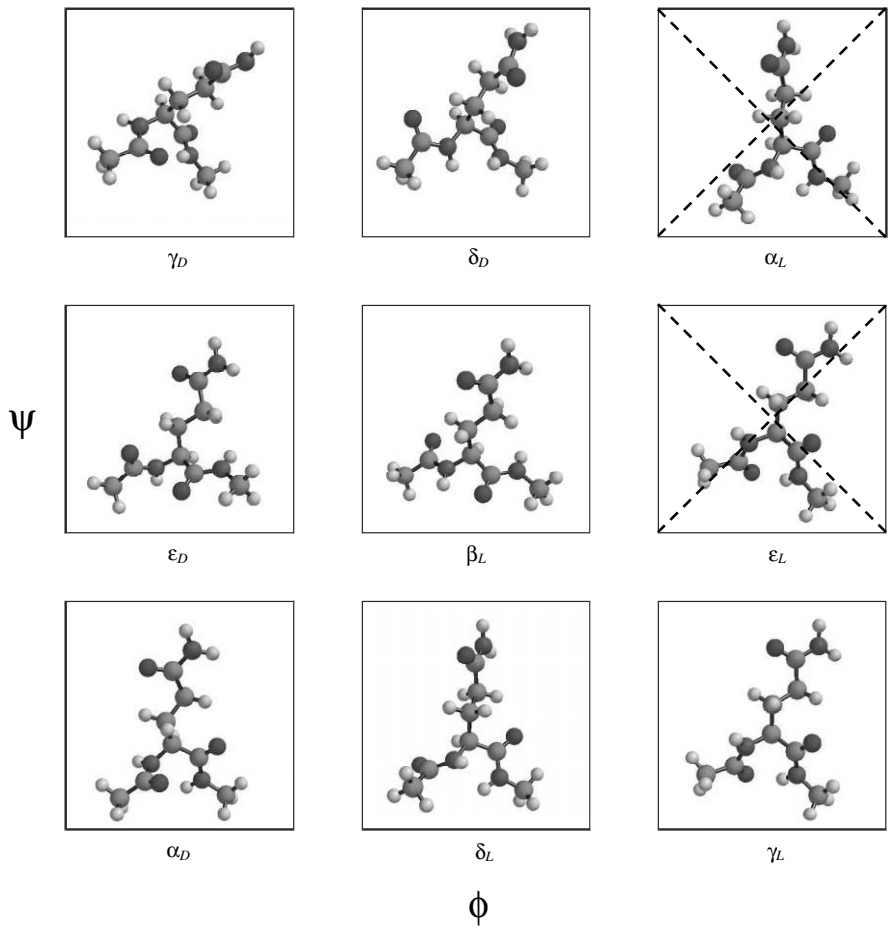

Fig. 6. Seven backbone conformers located on the Ramachandran PES.

(ϕ, ψ) and side-chain (χ_1, χ_2, χ_3) conformations. As far as the isomerism of the peptide bonds were concerned, the corresponding torsional angles (ω_0, ω_1) were optimized at about 180°:

$$-180^\circ \leq \phi \leq 180^\circ \quad (4a)$$

$$-180^\circ \leq \psi \leq 180^\circ \quad (4b)$$

$$-180^\circ \leq \chi_1 \leq 180^\circ \quad (4c)$$

$$-180^\circ \leq \chi_2 \leq 180^\circ \quad (4d)$$

$$-180^\circ \leq \chi_3 \leq 180^\circ \quad (4e)$$

2.2. Molecular computations

Ab initio computations were carried out at the RHF/3-21G level [14] of theory using the GAUSSIAN 98 program [15]. The total energies are given in hartrees, the relative energies and stabilization energies are given in kilocalories per mol (the usual conversion factor was used: 1 hartree = 627.5095 kcal mol^{-1}).

2.3. Stabilization energies

For the calculation of the stabilization energies, according to isodesmic reactions (Eq. (5)), the components' energy values have been summarized in Table 2.

$$\underset{\text{Reference conformation } \gamma_L \text{ or } \beta_L}{\text{MeCONH–CH}_2\text{–CONHMe}} + \text{CH}_3\text{–R} \rightarrow \underset{\text{conformation X}}{\text{MeCONH–CHR–CONHMe}} + \text{CH}_3\text{–H} \quad (5)$$

The stabilization energies are computed as follows:

$$\Delta E_{\text{stabilization}} = \{E[\text{MeCONH–CHR–CONHMe}]_x + E[\text{CH}_3\text{–H}]\} - \{E[\text{MeCONH–CH}_2\text{–CONHMe}]\gamma_L \text{ or } \beta_L + \text{CH}_3\text{–R}]\} \quad (6)$$

3. Results and discussion

3.1. Side-chain model: butanamide

In the first phase of the research, butanamide (**I**), a model side-chain for glutamine (**II**) was subject to conformational analysis. Of the three torsional angles the first one (χ_1) was omitted from consideration since the methyl group with its three equivalent hydrogens has only one unique stable conformation. Thus, the conformational problem of (**I**) is reduced (Eq. (7)) to a PES:

$$E_{\chi_1=\text{opt}} = E(\chi_2, \chi_3) \quad (7)$$

The computed conformational potential energy surface (Eq. (7)) is shown in two representations in Fig. 1. The results of regular (i.e. non-tight) optimizations are summarized in Table 3. It is interesting to note that the g^+a and g^-a conformations are slightly more stable than the *anti* conformation implying that the *gauche*-effect is operative.

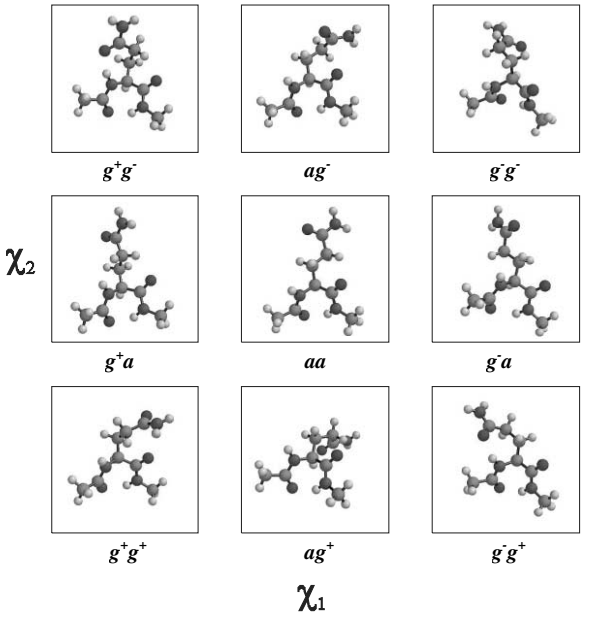

Fig. 7. Nine conformers located on the side-chain PES for γ_L backbone conformation. (Note: the γ_L (a,a) conformation is already shown in Fig. 6.)

It is relatively easy to demonstrate the principle of dynamic chirality [16] in the case of butanamide if we consider this molecule as 1,2-disubstituted ethane shown in (Eq. (8)) in its *syn* form:

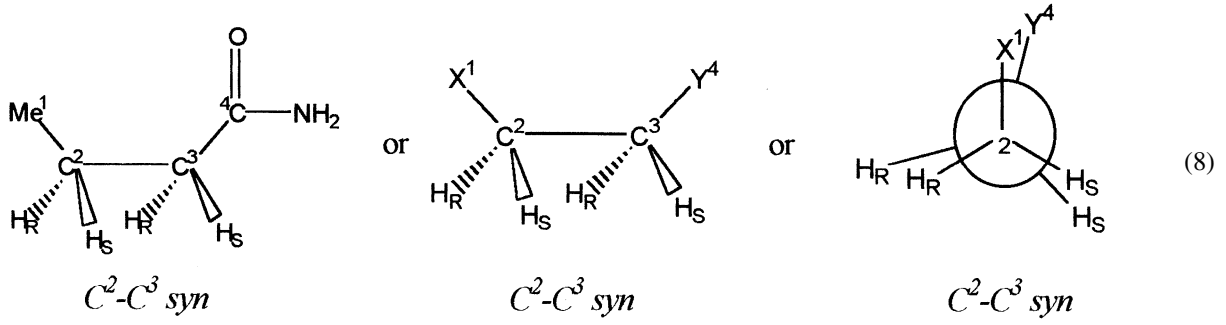

(8)

The pro-*R* hydrogens (H_R) and the pro-*S* hydrogens (H_S) are clearly indicated in these structures (Eq. (8)). Of the conformers in (Eq. (9)) the *anti* is symmetric, therefore C^2–H_R and C^2–H_S bond lengths are expected to be equal. The same observation is expected for C^3–H_R and C^3–H_S. In contrast to that, all four C–H bond lengths are

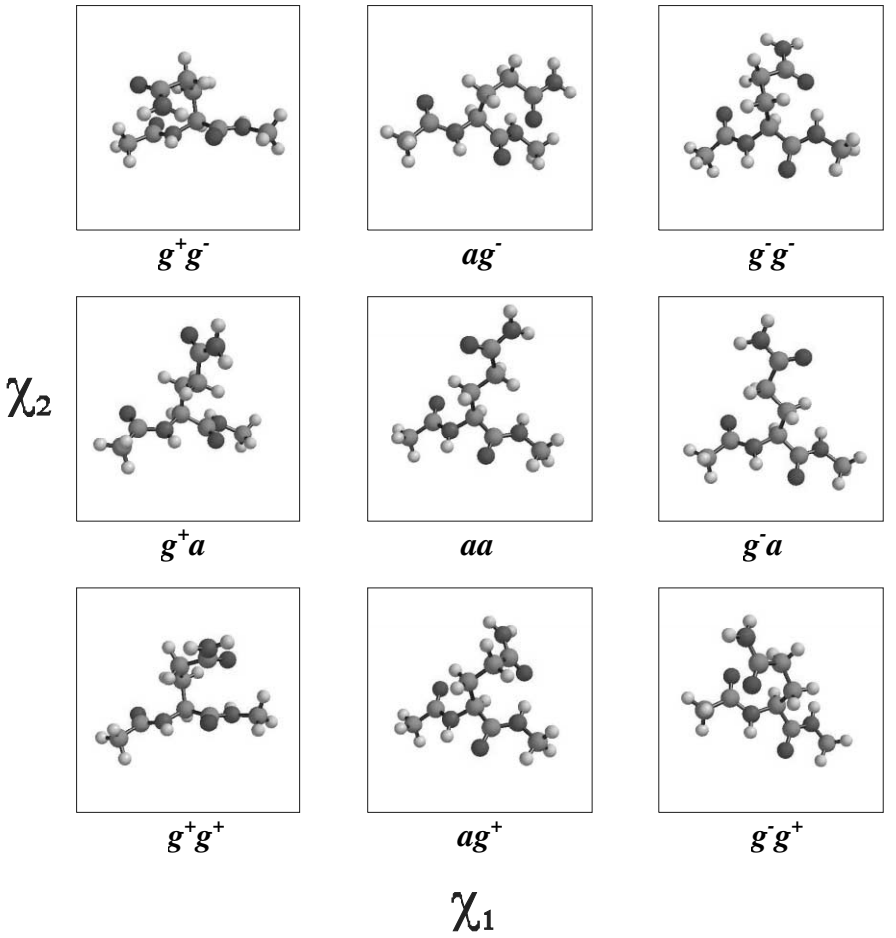

Fig. 8. Nine conformers located on the side-chain PES for the β_L backbone conformation. (Note: the β_L (a,a) conformation is already shown in Fig. 6.)

expected to be different for the g^+ and g^- conformers as shown by Eq. (9). The g^+ and g^- conformers are enantiomeric. This is the manifestation of axis chirality associated with the clockwise and counter-clockwise rotation about the C^2–C^3 bond:

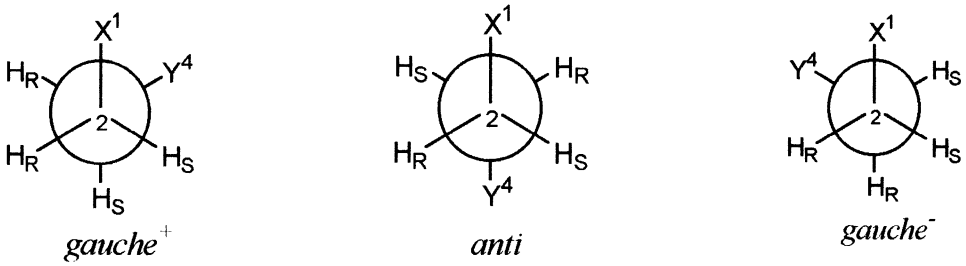

(9)

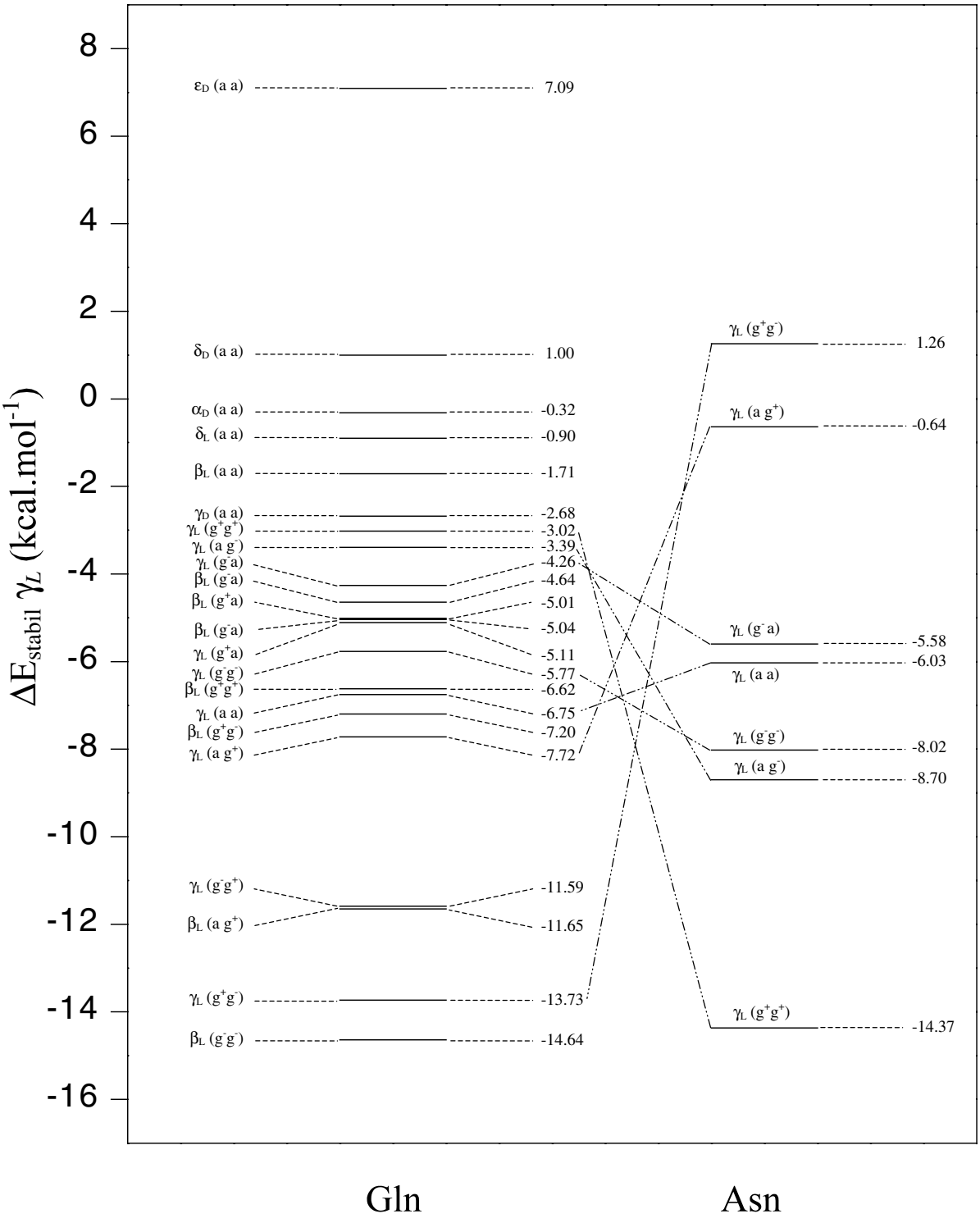

Fig. 9. A comparison of $\Delta E_{stabil}(\gamma_L)$ values obtained for glutamine (**II**) and asparagine (**IV**).

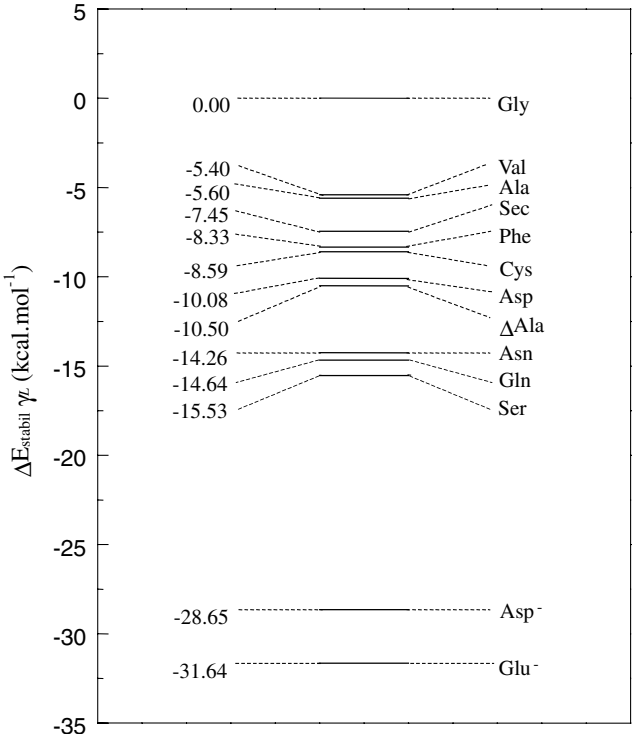

Fig. 10. A comparison of $\Delta E_{\text{stabil}}(\gamma_L)$ values obtained for various amino acid residues.

However, this axis chirality is expected to induce point chirality in C^2 as well as C^3 within the framework of dynamic chirality [16].

3.2. Peptide model: N-acetyl-L-glutamine-N-methylamide

According to Eq. (1), a PEHS can describe the side-chain orientation in the glutamine residue. If on the basis of the model compound's conformational analysis, we select only the $\chi_3 =$ *anti* orientation of the $-CONH_2$ moiety, then from the three-level PEHS (shown in Fig. 2) only the central level will be investigated.

For 19 out of the 20 amino acid residues [17–19], proline [19] being an exception, nine backbone (BB) conformations are expected to exist, as can be seen in Fig. 3A. However, for many of the peptides not all nine anticipated conformers appear as energy minima on the Ramachandran PES [17–19]. In many of the cases the α_L and ε_L conformations are annihilated [17–19]. For this reason, we made an exploratory study on the Ramachandran PES, $E(\phi, \psi)$, using fully *anti* conformations of the glutamine side-chain (cf. Fig. 3B) in all nine BB conformations. The PES is shown in Fig. 4 and the results of the geometry optimizations are summarized in Table 4.

The following observations can be made:

(i) The α_L and ε_L conformations, which are usually annihilated, here too, are not energy minima on the Ramachandran PES.
(ii) No other backbone conformations were annihilated on the Ramachandran PES.
(iii) All backbone conformations tolerate the a,a side-chain conformation.

Such observations are typical for most amino acids that have been already studied. The current database, which may provide the basis for comparison, includes the following N- and C-protected amino acids containing a *trans*-peptide bond: Gly [17,18,21–26],

Table 8
Values of side-chain C–H bond length of the two prochiral CH_2 moieties as in butanamide and *N*-acetyl-L-glutamine-*N*-methylamide in their various conformations

χ_1	χ_2	χ_3	C_2–H_{11}	C_2–H_{10}	C_3–H_{13}	C_3–H_{12}	C_7–H_{13}	C_7–H_{12}	C_8–H_{14}	C_8–H_{15}	χ_1	χ_2	χ_3	BB
							1.0866	1.0833	1.0790	1.0858	g^+	g^+	a	γ_L
							1.0811	1.0800	1.0818	1.0864	g^+	g^+	a	β_L
g^+	g^+	a	1.0844	1.0820	1.0857	1.0871	1.0823	1.0808	1.0771	1.0878	g^+	a	a	γ_L
							1.0805	1.0805	1.0862	1.0821	g^+	a	a	β_L
							1.0826	1.0831	1.0848	1.0878	g^+	g^-	a	γ_L
							1.0846	1.0802	1.0836	1.0791	g^+	g^-	a	β_L
							1.0819	1.0830	1.0811	1.0863	a	g^+	a	γ_L
							1.0810	1.0829	1.0790	1.0820	a	g^+	a	β_L
							1.0803	1.0812	1.0868	1.0844	a	a	a	β_L
							1.0808	1.0824	1.0877	1.0804	a	a	a	γ_L
							1.0812	1.0798	1.0892	1.0770	a	a	a	α_D
g^+	a	a	1.0822	1.0822	1.0865	1.0865	1.0803	1.0762	1.0893	1.0804	a	a	a	ε_D
							1.0805	1.0787	1.0863	1.0833	a	a	a	γ_D
							1.0779	1.0801	1.0841	1.0857	a	a	a	δ_D
							1.0810	1.0830	1.0876	1.0791	a	a	a	δ_L
							1.0828	1.0813	1.0853	1.0803	a	g^-	a	γ_L
							1.0810	1.0804	1.0869	1.0849	a	g^-	a	β_L
							1.0802	1.0809	1.0866	1.0840	g^-	g^+	a	γ_L
							1.0814	1.0838	1.0807	1.0864	g^-	g^+	a	β_L
g^+	g^-	a	1.0820	1.0844	1.0844	1.0871	1.0806	1.0807	1.0864	1.0835	g^-	a	a	γ_L
							1.0839	1.0803	1.0833	1.0834	g^-	a	a	β_L
							1.0827	1.0798	1.0848	1.0848	g^-	g^-	a	γ_L

Ala [17,18,21–26] Val [27], Phe [28,29] and Ser [30–32]. Preliminary studies have been published on Pro [20], Asp [33], Asn [34], Cys [35], and Sec (selenocysteine) [36].

In the next phase of our study, we have selected two backbone conformations, γ_L and β_L, to investigate the side-chain conformations. The optimized structures for the γ_L backbone are given in Table 5 and those for the β_L structure are summarized in Table 6.

3.3. Relative energies and side-chain backbone interactions

The various types of BB/BB and SC/BB interactions are presented in Fig. 5. A summary of the actual interactions, occurring in the 23 conformers studied, is presented in Table 7. This summary clearly shows that those conformers that are low in ΔE have several different types of interaction. The converse is also true; namely, conformers, which have only one interaction are considerably less stable. A graphical presentation of the 23 structures is shown in Figs. 6–8. In these figures, the structures are arranged in the pattern of their corresponding potential energy surfaces.

3.4. Stabilization energies

The stabilization energy of the side-chain exerted on the backbone of course varies from amino acid to amino acid. It also varies by conformation within a given amino acid. A comparison of the two amino acids with acidamide side-chains (i.e. asparagine and glutamine) are shown in Fig. 9.

The different protective groups (on the one hand HCO– and $–NH_2$ as well as MeCO– and –NHMe on the other hand) cause only a very small discrepancy. For the L-asparagine diamide at its global minimum, the $\Delta E_{stabil}(\gamma_L) = -14.259$ and -14.369 kcal mol^{-1} for the former and the latter case, respectively, at the RHF/3-21G level of theory. Thus, the difference is only 0.11 kcal mol^{-1}. Consequently, a comparison of the results obtained using two different sets of protective groups is quite acceptable. This point is important

because not all amino acids are reported in the literature with both sets of protective groups.

Fig. 10 compares the stabilization energies $\Delta E_{\text{stabil}(\beta_L)}$ for the global minimum of the various amino acids collected in the database [37].

3.5. Side-chain folding

Side-chain folding is not only interesting but also important for two reasons. On the one hand, side-chain orientation can influence backbone folding via side-chain–backbone interaction. On the other hand, side-chain folding can limit the biological function of the amino acid. The understanding of the phenomenon of side-chain folding requires relatively long aliphatic side-chains and there are only a few amino acids, which fulfil this requirement.

Glutamine has a long enough side-chain so the problem of side-chain folding may be explored. A folded chains, like butanamide, exhibits dynamic chirality unless it is in its fully symmetrical form (i.e. fully *anti*). In the case of the current amino acid residue, namely glutamine, no symmetric situation may exist because the side-chain is placed in an asymmetric environment due to the proximity of the α-carbon. Consequently, C–H_R and C–H_S bond lengths are expected to be different even in the a,a side-chain orientation. The numerical values of the C–H bond lengths for the various conformers of **I** and **II** are summarized in Table 8.

Acknowledgements

The authors wish to extend genuine thanks and appreciation for the great help of Kenneth P. Chasse (math@velocet.ca), Graydon Hoare (graydon@pobox.com) and Velocet Communications Inc. for CPU cycles, network support, database management and for the ongoing development of distributed processing. Special thanks are extended to Andrew M. Chasse (fixy@fixy.org) for his continuing and progressive integration of novel software techniques, hardware configurations and well-planned scripting and coding, each significantly reducing the necessary CPU time for each calculation.

This work was supported by grants from Universidad Nacional de San Luis (UNSL), and Consejo Nacional de Investigaciones Científicas y Técnicas (CONICET) of Argentina. R.D. Enriz is a carrier researcher of CONICET.

References

[1] K. Laki, L. Lorand, Science 108 (1948) 280.
[2] A.G. Loewy, C. Veneziale, M. Forman, Biochem. Biophys. Acta 26 (1957) 670.
[3] A.G. Loewy, K. Dunathan, K. Kriel, J. Wolfinger, J. Biol. Chem. 236 (1961) 2625.
[4] A.G. Loewy, A. Dahlberg, K. Dunathan, K. Kriel, J. Wolfinger, J. Biol. Chem. 236 (1961) 2634.
[5] A.G. Loewy, K. Dunathan, J.A. Gallant, J. Biol. Chem. 236 (1961) 2644.
[6] A.G. Loewy, J.A. Gallant, K. Dunathan, J. Biol. Chem. 236 (1961) 2648.
[7] Y. Sokata, N. Aoki, J. Clin. Invest. 65 (1980) 290.
[8] L. Muszbek, R. Adany, G. Szegedi, J. Polgar, M. Kavai, Thromb. Res. 37 (1985) 401.
[9] V.C. Yee, L. Pederseu, I. Letrong, P.D. Bishop, R.E. Stenkamp, D.C. Teller, Proc. Natl Acad. Sci. USA 91 (1994) 7296.
[10] L. Muszbek, V.C. Yee, Zs. Hevessy, Thromb. Res. 94 (1999) 271.
[11] J. Arnaud, M. Garriga, J. Sci. Food Agric. 80 (2000) 1655–1658.
[12] M.A. Berg, S.J. Salprieto, A. Perczel, Ö. Farkas, I.G. Csizmadia, J. Mol. Struct. (Theochem) 504 (2000) 127–139.
[13] IUPAC–IUB Commission on Biochemical Nomenclature, Biochemistry 9 (1970) 3471.
[14] J.S. Binkley, J.A. Pople, W.J. Hehre, J. Am. Chem. Soc. 102 (1980) 939.
[15] M.J. Frisch, G.W. Trucks, H.B. Schlegel, G.E. Scuseria, M.A. Robb, J.R. Cheeseman, V.G. Zakrzewski, J.A. Montgomery, Jr., R.E. Stratmann, J.C. Burant, S. Dapprich, J.M. Millam, A.D. Daniels, K.N. Kudin, M.C. Strain, O. Farkas, J. Tomasi, V. Barone, M. Cossi, R. Cammi, B. Mennucci, C. Pomelli, C. Adamo, S. Clifford, J. Ochterski, G.A. Petersson, P.Y. Ayala, Q. Cui, K. Morokuma, D.K. Malick, A.D. Rabuck, K. Raghavachari, J.B. Foresman, J. Cioslowski, J.V. Ortiz, A.G. Baboul, B.B. Stefanov, G. Liu, A. Liashenko, P. Piskorz, I. Komaromi, R. Gomperts, R.L. Martin, D.J. Fox, T. Keith, M.A. Al-Laham, C.Y. Peng, A. Nanayakkara, C. Gonzalez, M. Challacombe, P.M.W. Gill, B. Johnson, W. Chen, M.W. Wong, J.L. Andres, C. Gonzalez, M. Head-Gordon, E.S. Replogle, J.A. Pople, GAUSSIAN 98, Revision A.7, Gaussian, Inc., Pittsburgh, PA, 1998.
[16] G.A. Chasse, M.L. Mak, E. Deretey, Z. Szekely, A. Perczel, R.D. Enriz, I.G. Csizmadia, Conformationally induced stereo centres in small achiral single rotor molecules, submitted for publication.
[17] A. Perczel, J.G. Angyan, M. Rajtar, W. Viviani, J.L. Rivail, J.F. Marcoccia, I.G. Csizmadia, J. Am. Chem. Soc. 113 (1991) 6256–6265.
[18] M.A. McAllister, A. Perczel, P. Csaszar, W. Viviani, J.L. Rivail, I.G. Csizmadia, J. Mol. Struct. (Theochem) 288 (1993) 161–180.

[19] A. Perczel, I.G. Csizmadia, Int. Rev. Phys. Chem. 14 (1995) 127–168.
[20] H.A. Baldoni, A.M. Rodriguez, G. Zamarbide, R.D. Enriz, O. Farkas, P. Csaszar, L.L. Torday, C.P. Sosa, I. Jauli, A. Perczel, M. Hollosi, I.G. Csizmadia, J. Mol. Struct. (Theochem) 465 (1999) 79–91.
[21] S.J. Weiner, V.C. Singh, T.J. O'Donnell, P.A. Kollman, J. Am. Chem. Soc. 106 (1984) 6243.
[22] A.M. Sapse, L.M. Fugler, D. Cowburn, Int. J. Quantum Chem. 29 (1986) 1241.
[23] T.C. Chean, S. Krimm, J. Mol. Struct. (Theochem) 188 (1989) 15.
[24] T.C. Chean, S. Krimm, J. Mol. Struct. (Theochem) 193 (1989) 1.
[25] T. Head-Gordon, M. Head-Gordon, M.J. Frish, C. Brooks, J. Pople, Int. J. Quantum Chem. Quantum Biol. Symp. 16 (1989) 311.
[26] T. Head-Gordon, M. Head-Gordon, M.J. Frish, C. Brooks, J. Pople, J. Am. Chem. Soc. 113 (1991) 5989.
[27] W. Viviani, J.-L. Rivail, A. Perczel, I.G. Csizmadia, J. Am. Chem. Soc. 115 (1993) 8321.
[28] Ö. Farkas, M.A. McAllister, J.H. Ma, A. Perczel, M. Hollósi, I.G. Csizmadia, J. Mol. Struct. (Theochem) 369 (1996) 105.
[29] A. Perczel, Ö. Farkas, I.G. Csizmadia, Can. J. Chem. 75 (1997) 1120.
[30] Ö. Farkas, A. Perczel, J.F. Marcoccia, M. Hollósi, I.G. Csizmadia, J. Mol. Struct. (Theochem) 331 (1995) 27.
[31] A. Perczel, Ö. Farkas, I.G. Csizmadia, J. Comput. Chem. 17 (1996) 821.
[32] A. Perczel, Ö. Farkas, I.G. Csizmadia, J. Am. Chem. Soc. 118 (1996) 7809.
[33] S.J. Salpietro, A. Perczel, Ö. Farkas, R.D. Enriz, I.G. Csizmadia, J. Mol. Struct. (Theochem) 497 (2000) 39.
[34] M. Berg, S.J. Salpietro, I.G. Csizmadia, J. Mol. Struct. (Theochem) 504 (2000) 127.
[35] M.A. Zamora, H.A. Baldoni, J.A. Bombasaro, M.L. Mak, A. Perczel, Ö. Farkas, R.D. Enriz, J. Mol. Struct. (Theochem) 540 (2001) 271.
[36] J.C. Vank, C.P. Sosa, A. Perczel, I.G. Csizmadia, Can. J. Chem. 78 (2000) 395.
[37] G.A. Chasse, A.M. Rodríguez, M.L. Mak, E. Deretey, A. Perczel, C.P. Sosa, R.D. Enriz, I.G. Csizmadia, J. Mol. Struct. (Theochem) 537 (2001) 319.